Int. J. Heat Mass Transfer. Vol. 16, pp. 769–785. Pergamon Press 1973. Printed in Great Britain

MIXED CONVECTION ABOVE A HEATED HORIZONTAL SURFACE

C. A. HIEBER

Mechanical Engineering Department, Clarkson College of Technology, Potsdam, New York 13676, U.S.A.

(*Received* 17 *January* 1972 *and in revised form* 11 *August* 1972)

Abstract— Buoyancy effects are determined analytically for the laminar boundary-layer region above an isothermally heated, semi-infinite horizontal surface located in a horizontal uniform stream. The flow conditions are determined under which the boundary layer consists of a forced-flow-dominated near region and a buoyancy-dominated far region connected by an intermediate region in which forced and natural convection are of comparable magnitude. Perturbation expansions are obtained for the near and far regions with results for the intermediate region being obtained by graphical interpolation.

Although it is well-known that, at fixed Reynolds and Grashof number, the effect of buoyancy decreases monotonically as the Prandtl number increases, it is found for the present problem that, for fixed U_∞ and ΔT, the effect of natural convection in gases is not only more important than in large-σ oils but also than in small-σ liquid metals; this is attributable to the relatively small kinematic viscosity and coefficient of thermal expansion of liquid metals. In any case, if $\Delta T \lesssim 20°C$ then U_∞ must be quite small ($\lesssim 20$ cm/s) if buoyancy effects are to become significant before turbulent transition occurs.

Presentation of the theoretical results in terms of $G/R^{\frac{1}{2}}$ versus σ leads to a clear demarcation of the forced-convection, mixed-convection and natural-convection heat-transfer regimes.

NOMENCLATURE

g, gravitational acceleration (directed along negative y-axis);

G, local Grashof number $\equiv g\beta(T_w - T_\infty)\,x^3/\nu^2$;

N, local Nusselt number $\equiv -(x/\Delta T)\,(\partial T/\partial)_w$;

$\bar{N}$, average Nusselt number

$$\equiv (1/\Delta T)\int_0^x (-\partial T/\partial y)_w\,\mathrm{d}x;$$

R, local Reynolds number $\equiv U_\infty x/\nu \equiv x/\lambda$;

T, temperature;

U_∞, magnitude of uniform stream (directed along positive x-axis);

U_B, $\equiv (\nu/x)\,G^{\frac{1}{2}} \equiv U_\infty G^{\frac{1}{2}}/R$;

u, fluid velocity component in x-direction;

v, fluid velocity component in y-direction;

x, horizontal coordinate measured along plate;

y, vertical coordinate measured above plate.

Greek symbols

α, $= 0{\cdot}33206$;

β, coefficient of thermal expansion;

γ, $\equiv G/R^3 \equiv g\beta(T_w - T_\infty)\,\nu/U_\infty^3$;

Γ, gamma function;

δ, $\equiv (\lambda x)^{\frac{1}{2}} \equiv x/R^{\frac{1}{2}}$;

δ_B, $\equiv x/G^{\frac{1}{2}}$;

δ_{th}, $\equiv \Delta T/(-\partial T/\partial y)_w$;

δ^*, displacement thickness $\equiv \int_{B.L.} (1 - u/U_\infty)\,\mathrm{d}y$;

ΔT, $\equiv T_w - T_\infty$;

ε, $\equiv G/R^{\frac{1}{2}}$;

$\tilde{\varepsilon}$, $\equiv R/G^{\frac{1}{2}}$;

$\hat{\varepsilon}$, $\equiv G^{\frac{1}{2}}/(R\sigma^{\frac{1}{2}})$;

ε^*, $\equiv R^{\frac{1}{2}}\sigma^{\frac{1}{2}}/G^{\frac{1}{2}}$;

ζ; $\equiv \sigma^{\frac{1}{2}}\eta$;

$\tilde{\zeta}$, $\equiv \sigma^{\frac{1}{2}}\tilde{\eta}$;

η, $\equiv y/\delta$;
$\tilde{\eta}$, $\equiv y/\delta_B$;
κ, $\equiv \sigma^{\frac{1}{4}}\tilde{\eta}$;
λ, $\equiv \nu/U_\infty$ ("viscous length");
ν, kinematic viscosity;
ξ, $\equiv \sigma^{\frac{1}{3}}\eta$;
$\tilde{\xi}$, $\equiv \sigma^{-\frac{1}{15}}\tilde{\eta}$;
ρ, density of fluid;
σ, Prandtl number;
χ, $\equiv G/R^{\frac{5}{2}} \equiv \gamma R^{\frac{1}{2}}$;
ψ, streamfunction;
ω, $\equiv \sigma^{-\frac{1}{15}}\tilde{\eta}$.

Subscripts

B, buoyancy-induced;
F, forced-flow-induced;
w, value at wall;
∞, value of undisturbed fluid.

1. INTRODUCTION

A THEORETICAL investigation is made of the laminar boundary-layer region existing above an isothermally heated, semi-infinite horizontal plate located in a horizontal uniform stream. This is the analogue of the vertical-plate problem considered by Szewczyk [1] and Merkin [2].

The structure of the boundary layer is characterized by the Prandtl number (σ) and the mixed-convection parameter, $\gamma \equiv G/R^3 = g\beta\Delta T\nu/U_\infty^3$. In particular, it is shown that the buoyant effect is dominant throughout the boundary layer unless γ is sufficiently small, namely, $\gamma \ll 1$ when $\sigma = 0(1)$, $\gamma < 0(\sigma^{\frac{1}{3}})$ as $\sigma \to \infty$ and $\gamma < 0(\sigma)$ as $\sigma \to 0$. If γ satisfies this condition then the boundary layer consists of a forced-flow-dominated near region and a buoyancy-dominated far region which are connected by an intermediate region in which both effects are comparable.

The above "near region" was investigated by Mori [3] and Sparrow and Minkowycz [4] for particular values of σ. The "far region" has not been studied previously although the leading problem in this region is that of pure natural convection, which was investigated by Stewartson [5] and Gill *et al.* [6] for particular values of σ, and by Rotem and Claassen [7] for $\sigma \to \infty$ and $\sigma \to 0$.

In sections 2–4, a detailed analysis is made for the cases $\sigma = 0(1)$, $\sigma \to \infty$ and $\sigma \to 0$, respectively, with primary attention being given to when γ satisfies the above condition, this being the least trivial and most interesting situation. The results of sections 2–4 are discussed and applied in section 5.

2. PRANDTL NUMBER OF 0(1)

Assuming the forced flow to be dominant in some region of the boundary layer (the required flow conditions to be determined aposteriori), then, as was shown by Mori [3] and Sparrow and Minkowycz [4], appropriate expansions for the stream function and temperature in this region are given by:

$$\left.\begin{aligned} \psi &= U_\infty\delta[F_0(\eta) + \sum_{m=1}^{\infty} \varepsilon^m F_m(\eta;\sigma)], \\ T - T_\infty &= \Delta T \sum_{m=0}^{\infty} \varepsilon^m H_m(\eta;\sigma), \end{aligned}\right\} \quad (1)$$

where the governing equations and boundary conditions for the various terms are given by:

$$F_0''' + \tfrac{1}{2}F_0F_0'' = 0; \quad F_0(0) = 0 = F_0'(0), \quad F_0'(\infty) = 1, \quad (2)$$

$$H_0'' + \tfrac{1}{2}\sigma F_0H_0' = 0; \quad H_0(0) = 1, \quad H_0(\infty) = 0, \quad (3)$$

$$\left.\begin{aligned} &F_m''' + \tfrac{1}{2}F_0F_m'' - \frac{m}{2}F_0'F_m' + \frac{m+1}{2}F_0''F_m \\ &\quad = -\frac{m}{2}\int_\eta^\infty H_{m-1}\,d\eta - \tfrac{1}{2}\eta H_{m-1} + Q_m, \\ &F_m(0) = 0 = F_m'(0) = F_m'(\infty), \qquad (m \geqslant 1) \end{aligned}\right\} \quad (4)$$

$$\left.\begin{aligned} &\frac{1}{\sigma}H_m'' + \tfrac{1}{2}F_0H_m' - \frac{m}{2}F_0'H_m \\ &\qquad + \frac{m+1}{2}H_0'F_m = S_m, \\ &H_m(0) = 0 = H_m(\infty), \qquad (m \geqslant 1) \end{aligned}\right\} \quad (5)$$

where

$$Q_1 = 0 = S_1, \quad Q_2 = \tfrac{1}{2}F_1'F_1' - F_1F_1'',$$
$$S_2 = \tfrac{1}{2}F_1'H_1 - F_1H_1',$$
$$Q_3 = \tfrac{3}{2}F_1'F_2' - F_1F_2'' - \tfrac{3}{2}F_1''F_2,$$
$$S_3 = F_1'H_2 - F_1H_2' + \tfrac{1}{2}F_2'H_1 - \tfrac{3}{2}F_2H_1', \ldots,$$

and $u = \partial\psi/\partial y$, $v = -\partial\psi/\partial x$.

The above equations are based upon the usual Boussinesq approximation together with the assumptions of constant transport properties and negligible viscous dissipation. F_0 is the well-known Blasius stream-function and H_0 is the associated forced-flow temperature. The higher-order velocity components are due to buoyancy via the first two terms on the right hand side of (4); these latter terms represent a favorable horizontal pressure gradient which arises from a hydrostatic force balance in the vertical direction combined with an x-dependent temperature (hence, density) distribution.

In order that the above expansion be self-consistent, it is necessary that the boundary layer be thin, i.e. $\delta \ll x$, and that the buoyancy effect be small, i.e. $\varepsilon \ll 1$. The first constraint can be rewritten as $1 \ll (x/\lambda)^{\frac{1}{4}}$ and, the latter, as $(x/\lambda)^{\frac{1}{4}} \ll \gamma^{-1}$. Hence, in order that such a region exist, it is necessary that $1 \ll \gamma^{-1}$.

Therefore, if $\gamma \ll 1$, the expansions in (1) are applicable in the region $0(1) < x/\lambda < 0(\gamma^{-2})$, with the buoyancy becoming a leading-order effect where $x/\lambda = 0(\gamma^{-2})$, and, by implication, the dominant effect where $x/\lambda > 0(\gamma^{-2})$.

Similarly, a formal perturbation expansion about the natural-convection flow results in:

$$\left.\begin{aligned} \psi &= U_B\delta_B \sum_{m=0}^{\infty} \tilde{\varepsilon}^m \tilde{F}_m(\tilde{\eta};\sigma), \\ T - T_\infty &= \Delta T \sum_{m=0}^{\infty} \tilde{\varepsilon}^m \tilde{H}_m(\tilde{\eta};\sigma), \end{aligned}\right\} \quad (6)$$

with the governing equations and boundary conditions for the various terms being given by:

$$\left.\begin{aligned} &\tilde{F}_0''' + \tfrac{3}{5}\tilde{F}_0\tilde{F}_0'' - \tfrac{1}{5}\tilde{F}_0'\tilde{F}_0' \\ &\qquad = -\tfrac{2}{5}\int_{\tilde{\eta}}^{\infty} \tilde{H}_0 \, d\tilde{\eta} - \tfrac{2}{5}\tilde{\eta}\tilde{H}_0, \\ &\frac{1}{\sigma}\tilde{H}_0'' + \tfrac{3}{5}\tilde{F}_0\tilde{H}_0' = 0, \\ &\tilde{F}_0(0) = 0 = \tilde{F}_0'(0) = \tilde{F}_0'(\infty) = \tilde{H}_0(\infty), \\ &\qquad \tilde{H}_0(0) = 1, \end{aligned}\right\} \quad (7)$$

$$\left.\begin{aligned} &\tilde{F}_m''' + \tfrac{3}{5}\tilde{F}_0\tilde{F}_m'' + \frac{m-2}{5}\tilde{F}_0'\tilde{F}_m' + \frac{3-m}{5}\tilde{F}_0''\tilde{F}_m \\ &\qquad = \frac{m-2}{5}\int_{\tilde{\eta}}^{\infty} \tilde{H}_m \, d\tilde{\eta} - \tfrac{2}{5}\tilde{\eta}\tilde{H}_m + \tilde{Q}_m, \\ &\frac{1}{\sigma}\tilde{H}_m'' + \tfrac{3}{5}\tilde{F}_0\tilde{H}_m' + \frac{m}{5}\tilde{F}_0'\tilde{H}_m \\ &\qquad + \frac{3-m}{5}\tilde{H}_0'\tilde{F}_m = S_m, \qquad (m \geqslant 1) \\ &\tilde{F}_m(0) = 0 = \tilde{F}_m'(0) = \tilde{H}_m(0) = \tilde{H}_m(\infty), \\ &\qquad \tilde{F}_m'(\infty) = \delta_{1m} \end{aligned}\right\} \quad (8)$$

where

$$\tilde{Q}_1 = 0 = \tilde{S}_1, \quad \tilde{Q}_2 = -\tfrac{2}{5}\tilde{F}_1\tilde{F}_1'',$$
$$\tilde{S}_2 = -\tfrac{1}{5}\tilde{F}_1'\tilde{H}_1 - \tfrac{2}{5}\tilde{F}_1\tilde{H}_1',$$
$$\tilde{Q}_3 = -\tfrac{3}{5}\tilde{F}_1'\tilde{F}_2' - \tfrac{2}{5}\tilde{F}_1\tilde{F}_2'' - \tfrac{1}{5}\tilde{F}_2\tilde{F}_1'',$$
$$\tilde{S}_3 = -\tfrac{2}{5}(\tilde{F}_1\tilde{H}_2)' - \tfrac{1}{5}(\tilde{F}_2\tilde{H}_1)'.$$

That is, $\tilde{F}_0$ and $\tilde{H}_0$ correspond to the natural-convection problem considered by Stewartson [5], Gill *et al.* [6] and Rotem and Claassen [7], whereas the higher-order terms arise from the forced flow via the uniform-stream boundary condition, $\tilde{F}_1'(\infty) = 1$.

In order that the expansion in (6) be self-consistent, it is necessary that the boundary layer be thin, i.e. $\delta_B \ll x$, and that the forced-flow effect be small, i.e. $\varepsilon \ll 1$. The first constraint can be rewritten as $\gamma^{-\frac{1}{4}} \ll (x/\lambda)^{\frac{1}{4}}$ and, the latter, as $\gamma^{-\frac{1}{2}} \ll (x/\lambda)^{\frac{1}{4}}$.

If $\gamma \ll 1$, the second constraint is the more restrictive. It follows that, for the case $\gamma \ll 1$, (6)

is applicable to the region $0(\gamma^{-2}) < x/\lambda$, as expected.

If $\gamma = 0(1)$, expansion (1) is not applicable to any region of the flow whereas expansion (6) applies where $0(1) < x/\lambda$. That is, the buoyancy effect becomes dominant during the early development of the boundary layer and remains dominant throughout the boundary-layer region.

Lastly, if $\gamma > 0(1)$ then (1) is again nowhere-applicable whereas (6) applies where $\gamma^{-\frac{1}{4}} \ll (x/\lambda)^{\frac{3}{4}}$, i.e. $0(\gamma^{-\frac{1}{4}}) < x/\lambda$. Hence, the more restrictive constraint on (6) in this case concerns "$\delta_B \ll x$" rather than "$\tilde{\varepsilon} \ll 1$", implying that natural convection becomes dominant well before the boundary layer develops, the forced flow remaining a small effect throughout the boundary-layer region.

It is seen that, unless γ is sufficiently small, the mixed-convection phenomenon is degenerate in the boundary-layer region. Hence, unless stated otherwise, the remainder of the present analysis is directed towards the case in which a forced-flow-dominated boundary-layer region exists.

Numerical results at $\sigma = 0{\cdot}72$ for the first three terms in each of expansions (1) and (6) are as follows:

$$\left.\begin{aligned} F_0''(0) &= 0{\cdot}33206, \quad F_1''(0) = 1{\cdot}6971, \\ &\qquad F_2''(0) = -4{\cdot}9985, \\ H_0'(0) &= -0{\cdot}29564, \quad H_1'(0) = -0{\cdot}35574, \\ &\qquad H_2'(0) = 1{\cdot}5858, \end{aligned}\right\} \quad (9)$$

$$\left.\begin{aligned} \tilde{F}_0''(0) &= 0{\cdot}97840, \quad \tilde{F}_1''(0) = 0{\cdot}044271, \\ &\qquad \tilde{F}_2''(0) = 0{\cdot}15048, \\ \tilde{H}_0'(0) &= -0{\cdot}35741, \quad \tilde{H}_1'(0) = -0{\cdot}036910, \\ &\qquad \tilde{H}_2'(0) = -0{\cdot}019857, \end{aligned}\right\} \quad (10)$$

where the first two terms in (1) and the first term in (6) have been obtained previously.

Additional terms in (1) could be obtained in a straightforward but tedious manner. However, in obtaining additional terms in (6), a complication would arise at $m = 5$ due to the fact that the fifth-order homogeneous problem, equation (8) with $m = 5$ and $\tilde{Q}_5 \equiv 0 \equiv \tilde{S}_5$, has a non-trivial solution, namely, any multiple of

$$\tilde{F}_{5C} = \tilde{\eta}\tilde{F}_0' - \tfrac{3}{2}\tilde{F}_0, \quad \tilde{H}_{5C} = \tilde{\eta}\tilde{H}_0'.$$

Hence, following Stewartson [8], it would be necessary to introduce a term of order $\tilde{\varepsilon}^5 \log \tilde{\varepsilon}$ in expansion (6) and, in order to eliminate the indeterminacy (i.e. the arbitrary multiple of $\tilde{F}_{5C}, \tilde{H}_{5C}$) in the $0(\tilde{\varepsilon}^5)$ term, it would be necessary to integrate the full parabolic boundary-layer equations, starting from the near region. This procedure was followed by Merkin [2] in analyzing the vertical-plate case, for which the indeterminancy arises at $m = 2$. For the present case, accurate results may be obtained by an alternative procedure, as is shown shortly.

Based upon the preceding, the local Nusselt number for when $\sigma = 0{\cdot}72$ and $\gamma \ll 1$ is given by:

$$\frac{N}{R^{\frac{1}{4}}} = \begin{cases} 0{\cdot}29564 + 0{\cdot}35574\chi - 1{\cdot}5858\chi^2 \\ \qquad + 0(\chi^3), \quad \gamma \ll \chi \ll 1, \\ 0{\cdot}35741\chi^{\frac{1}{4}} + 0{\cdot}036910\,\chi^{-\frac{1}{4}} \\ \qquad + 0{\cdot}019857\chi^{-\frac{3}{4}} + 0(\chi^{-\frac{7}{4}}), \quad 1 \ll \chi \end{cases} \quad (11)$$

where $\chi \equiv G/R^{\frac{3}{4}} = \gamma R^{\frac{1}{4}}$. The $0(\chi^{-1})$ term in the second equation of (11) has been omitted since $\tilde{H}_3'(0) = 0$, as can be seen by noting that the third-order energy equation in (8) is an exact differential which, upon integration once and application of the thermal boundary condition at $\tilde{\eta} = \infty$, results in

$$(1/\sigma)\tilde{H}_3' = -\tfrac{3}{5}\tilde{F}_0\tilde{H}_3 - \tfrac{2}{5}\tilde{F}_1\tilde{H}_2 - \tfrac{1}{5}\tilde{F}_2\tilde{H}_1,$$

giving the above result since $\tilde{F}_n(0) = 0$ $(n \geqslant 0)$.

On the other hand, calculation of the total heat-transfer rate (per unit depth) from the surface extending between the leading edge and the local value of x results in:

$$\dot{Q} = \int_0^x k\left(-\frac{\partial T}{\partial y}\right)_{y=0} \mathrm{d}x = 2k\Delta T\gamma^{-1}\int_0^\chi p(t)\,\mathrm{d}t \quad (12)$$

where the asymptotic behavior of $p(\chi)$ for small and large χ is given by the right-hand side of (11).

Clearly, in order to evaluate the integral in (12), it is necessary also to know the behavior of $p(\chi)$ for when $\chi = 0(1)$ which, in turn, requires employing a finite-difference procedure such as that used by Merkin. Fortunately, as is shown below, the value of $\int_0^\infty p(\chi)\,d\chi$ can be determined from global energy considerations; in combination with the asymptotic behavior of $p(\chi)$ for small and large χ, it is then possible, via graphical means, to get a fairly good approximation to $p(\chi)$ for all χ.

Employing a global energy-rate balance, it is clear that the result for $\dot{Q}$ as obtained from (12) must equal the total thermal convection,

$$\rho C_p \int_{\text{B.L.}} u(T - T_\infty)\,dy.$$

In particular, if $\chi \gg 1$, the latter integral can be evaluated directly from the $\tilde{F}_n'$ and $\tilde{H}_n$, resulting in:

$$\left.\begin{aligned} \dot{Q} &= k\,\Delta T\,\gamma^{-1}\sigma[a_0\chi^{\frac{1}{2}} + a_1\chi^{\frac{1}{4}} + a_2\chi^{\frac{1}{4}} \\ &\qquad + a_3 + 0(\chi^{-\frac{1}{2}})], \\ a_m &= \int_0^\infty \Big(\sum_{k=0}^{m} \tilde{F}_k'\tilde{H}_{m-k}\Big)\,d\tilde{\eta}, \qquad m = 0, 1, 2, 3. \end{aligned}\right\} \tag{13}$$

For $\sigma = 0{\cdot}72$, evaluation of the integrals results in:

$$a_0 = 0{\cdot}82734, \quad a_1 = 0{\cdot}12816,$$
$$a_2 = 0{\cdot}13790, \quad a_3 = 0{\cdot}3165.$$

It is noted that, to within the numerical accuracy, $a_n = -[5/((3 - n)(0{\cdot}72))]\tilde{H}_n'(0), n = 0, 1, 2$. Introducing $q(\chi) \equiv p(\chi) - (0{\cdot}35741\chi^{\frac{1}{2}} + 0{\cdot}036910\chi^{-\frac{1}{4}} + 0{\cdot}019857\chi^{-\frac{3}{4}})$ and equating (12) and (13) results in:

$$\int_0^\chi q(t)\,dt = \tfrac{1}{2}(0{\cdot}72)\,a_3 + 0(\chi^{-\frac{1}{2}}) \qquad \text{as} \quad \chi \to \infty.$$

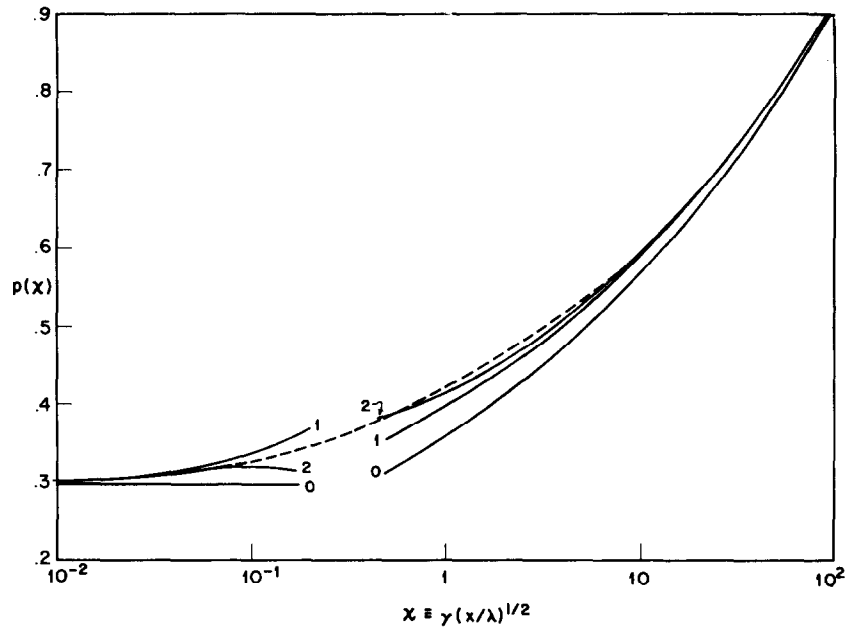

FIG. 1. Variation of $p(\chi)$ with χ for $\sigma = 0{\cdot}72$. Based upon equations (11) and (14).

Hence,

$$\int_0^\infty q(\chi)\,d\chi = 0{\cdot}1139. \tag{14}$$

The above results are displayed in Fig. 1, in which are shown zeroth-, first- and second-order approximations to $p(\chi)$ in the near and far regions. Making use of these curves, together with (14) and the asymptotic behavior, $q(\chi) = 0(\chi^{-\frac{3}{2}})$ as $\chi \to \infty$, $p(\chi)$ has been drawn in for any χ (dashed curve).

From the above it follows that, in the far region, the average Nusselt number between the leading edge and the local value of x is given by

$$\frac{\bar{N}}{R^{\frac{1}{2}}} = 0{\cdot}59568\chi^{\frac{1}{2}} + 0{\cdot}09228\chi^{-\frac{1}{2}} + 0{\cdot}09929\chi^{-\frac{3}{2}} + 0{\cdot}2278\chi^{-1} + 0(\chi^{-\frac{5}{2}}) \tag{15}$$

for when $\sigma = 0{\cdot}72$. It is noted that the $0(\chi^{-1})$ term in (15) does not arise from a local heat transfer in the far region but, rather, represents the integrated heat-transfer rate of the $\chi \leqslant 0(1)$ region. Indeed, had the $0(\chi^{-1})$ term in the far-region expansion of (11) been non-zero, it would have led to a term of $0(\chi^{-1}\log\chi)$ in (15). What is particularly interesting is the fact that the far-region expansion explicitly contains the net heat-transfer effect of the near region. This circumstance is analogous to the forced-flow velocity boundary layer for which Imai [9] showed, via global momentum considerations, that the drag of the "leading-edge region", $x/\lambda \leqslant 0(1)$, is explicitly contained within the boundary-layer expansion.

Concerning the effect of the leading-edge region upon the heat transfer in the present problem, it is noted that the near-region expansion of (11) does not apply where $\chi \leqslant 0(\gamma)$, i.e. in the leading-edge region where the boundary-layer approximation is not valid. However, an order-of-magnitude analysis shows that the contribution to $\dot{Q}$ by the region $x/\lambda \leqslant 0(1)$ is, at most, of order $k\Delta T$, which, from (13), is seen to be $0(\gamma)$ smaller than the heat-transfer rate from the near-region boundary layer.

If $\gamma \geqslant 0(1)$ then the upper equation in (11) is vacuous and the lower equation is applicable throughout the boundary-layer region, i.e. where $0(\gamma^{-\frac{1}{2}}) < x/\lambda$. In this case, higher-order boundary-layer effects, appearing as powers of $\delta_B/x = G^{-\frac{1}{4}}$, should be included in equation (6). This is clear on a physical basis since, as $\gamma \to \infty$ (interpreted as $U_\infty \to 0$, say), the forced-flow effect in (6) must vanish uniformly whereas the higher-order boundary-layer effects remain non-negligible in the early-development stage of the boundary layer. This matter will not be pursued further, however, since the present concern is with the mixed-convection phenomenon.

3. LARGE σ

The analysis of the large- and small-σ limits in the present and succeeding sections is confined to the first two terms in each of the near and far regions. Since the limiting behavior of the predominant term has been obtained previously, the present analysis is concerned with the first-order perturbation term.

In examining the flow for large-σ fluids, it is noted that the well-known limit of H_0 is:

$$H_0(\eta;\sigma) \begin{cases} \dfrac{(9\alpha/4)^{\frac{1}{3}}}{\Gamma(\frac{1}{3})}\displaystyle\int_\xi^\infty e^{-\alpha t^3/12}\,dt, \\ \qquad\qquad \xi \text{ fixed as } \sigma \to \infty \\ 0, \qquad \eta \text{ fixed as } \sigma \to \infty \end{cases} \tag{16}$$

where $\xi \equiv \sigma^{\frac{1}{3}}\eta$, $\alpha \equiv F_0''(0) = 0{\cdot}33206$ and Γ denotes the gamma function. Hence, the favorable horizontal pressure gradient on the right hand side of (4) is confined to the thin thermal boundary layer corresponding to $\eta = 0(\sigma^{-\frac{1}{3}})$. In this inner layer, the streamfunction of the buoyancy-induced velocity field is given by:

$$F_1(\eta;\sigma) \sim \sigma^{\frac{1}{3}}\Phi_1(\xi), \quad \xi \text{ fixed as } \sigma \to \infty \tag{17}$$

where

$$\left.\begin{aligned} \Phi_1'' &= -\tfrac{1}{2}\int_\xi^\infty \Theta_0\,d\xi - \tfrac{1}{2}\xi\Theta_0, \\ \Phi_1(0) &= 0 = \Phi_1'(0) = \Phi_1''(\infty). \end{aligned}\right\} \tag{18}$$

$\Theta_0(\xi)$ being the inner temperature distribution of (16). That is, the horizontal momentum balance in the inner layer is between the viscous diffusion and the buoyancy-induced pressure gradient, the inertial effect being $0(\sigma^{-1})$ smaller. Based on (17), it is noted that $u_B = 0(\varepsilon U_\infty/\sigma)$.

A closed-form solution for Φ_1 is given by

$$\Phi_1(\xi) = \frac{(3/2\alpha)^{\frac{1}{3}}}{\Gamma(\frac{1}{3})}\left\{\frac{\xi^3}{3}\int_\xi^\infty t^{-2}\,e^{-xt\xi/12}\,dt + \xi \times \int_0^\xi e^{-\alpha t\xi/12}\,dt - \frac{2}{3}\int_0^\xi t\,e^{-\alpha t^3/12}\,dt\right\}, \quad (19)$$

which results in

$$\Phi_1''(0) = \frac{(12/\alpha)^{\frac{1}{3}}}{2\Gamma(\frac{1}{3})},$$

$$\Phi_1(\xi) \underset{\xi\to\infty}{\sim} \frac{1}{\alpha}\xi - \left(\frac{32}{9\alpha^4}\right)^{\frac{1}{3}}\frac{\Gamma(\frac{2}{3})}{\Gamma(\frac{1}{3})}. \quad (20)$$

Hence, at the outer edge of the inner layer, u_B approaches the constant value $\varepsilon U_\infty/(\alpha\sigma)$, thereby necessitating an outer layer. In the latter, we have:

$$F_1(\eta;\sigma) \sim \sigma^{-1}\phi_1(\eta), \quad \eta \text{ fixed as } \sigma\to\infty, \quad (21)$$

where:

$$\left.\begin{aligned} &\phi_1''' + \tfrac{1}{2}F_0\phi_1'' - \tfrac{1}{2}F_0'\phi_1' + F_0''\phi_1 = 0,\\ &\phi_1'(\infty) = 0 = \phi_1(0), \quad \phi_1'(0) = \alpha^{-1}. \end{aligned}\right\} \quad (22)$$

That is, the horizontal momentum balance in the outer layer is between viscous and inertial effects, the flow being driven by the inner layer as evidenced by the inhomogeneous matching condition in (22).

As may be verified readily, the solution to (22) is simply

$$\phi_1(\eta) = \alpha^{-2}F_0'(\eta).$$

Hence, in particular, $\phi_1''(0) = \alpha^{-2}F_0'''(0) = 0$, which indicates that the momentum in the outer layer is not due to viscous shearing by the inner layer but, rather, as is seen by integrating (22),

$$\int_0^\infty F_0'\phi_1'\,d\eta = \tfrac{1}{2}F_0'(\infty)\,\phi_1(\infty) = \tfrac{1}{2}\phi_1(\infty),$$

i.e. the inertia associated with u_B in the outer layer is supplied by the x-momentum (U_∞ per unit mass) of the influx at its outer edge.

In a similar manner, one finds that

$$H_1(\eta;\sigma) \sim \begin{cases} \sigma^{-\frac{1}{3}}\Theta_1(\xi), & \xi \text{ fixed as } \sigma\to\infty,\\ 0, & \eta \text{ fixed as } \sigma\to\infty, \end{cases} \quad (23)$$

where

$$\left.\begin{aligned} &\Theta_1'' + \frac{\alpha}{4}\xi^2\Theta_1' - \frac{\alpha}{2}\xi\Theta_1 = -\Theta_0'\Phi_1,\\ &\Theta_1(0) = 0 = \Theta_1(\infty), \end{aligned}\right\} \quad (24)$$

Θ_1 being driven by the inhomogeneous right-hand side which represents the thermal convection of the forced-flow temperature by the buoyancy-induced velocity.

The solution to (24) is expressible in closed-form as:

$$\Theta_1(\xi) = \frac{(12/\alpha)^{\frac{1}{3}}}{\Gamma(\frac{1}{3})}\left\{h_2(\xi)\left[c - \int_0^\xi h_1\Phi_1\,d\xi\right] - h_1(\xi)\int_\xi^\infty h_2\Phi_1\,d\xi\right\}, \quad (25)$$

where $c = (h_1(0)/h_2(0))\int_0^\infty h_2\Phi_1\,d\xi$ and h_1, h_2 are linearly independent homogeneous integrals of (24) such that, as $\xi\to\infty$,

$$h_1(\xi) \sim \xi^2, \quad h_2(\xi) \sim \xi^{-4}\,e^{-\alpha\xi^2/12}.$$

In particular,

$$\Theta_1'(0) = -\frac{(9\alpha/4)^{\frac{1}{3}}}{\Gamma(\frac{1}{3})\,h_2(0)}\int_0^\infty h_2\Phi_1\,d\xi = -0{\cdot}59649. \quad (26)$$

In the far region, as was shown by Rotem and Claassen [7], $\tilde{H}_0$ is zero except for a thin thermal

boundary layer corresponding to $\tilde{\eta} = 0(\sigma^{-\frac{1}{4}})$ wherein the x-momentum balance for $\tilde{F}_0$ is between viscous diffusion and a buoyancy-induced favorable pressure gradient; in the outer boundary layer, corresponding to $\tilde{\eta} = 0(\sigma^{\frac{1}{16}})$, the viscous and inertial effects balance and the pressure gradient is zero.

Appropriate asymptotic expansions for (6) are given in the inner layer by:

$$\left.\begin{aligned} \psi &\sim U_B \delta_B \sigma^{-\frac{1}{4}}[\tilde{\Phi}_0(\kappa) \\ &\quad + \tilde{\varepsilon}\sigma^{\frac{1}{16}}\tilde{\Phi}_1(\kappa) + \ldots], \\ T - T_\infty &\sim \Delta T[\tilde{\Theta}_0(\kappa) \\ &\quad + \tilde{\varepsilon}\sigma^{\frac{1}{16}}\tilde{\Theta}_1(\kappa) + \ldots], \end{aligned}\right\} \begin{array}{l} \kappa \text{ fixed} \\ \text{as } \sigma \to \infty \end{array} \tag{27}$$

and, in the outer layer, by:

$$\left.\begin{aligned} \psi &\sim U_B \delta_B \sigma^{-\frac{1}{16}}[\tilde{\phi}_0(\omega) \\ &\quad + \tilde{\varepsilon}\sigma^{\frac{1}{4}}\tilde{\phi}_1(\omega) + \ldots], \\ T - T_\infty &\sim 0. \end{aligned}\right\} \begin{array}{l} \omega \text{ fixed} \\ \text{as } \sigma \to \infty \end{array} \tag{28}$$

Hence, $u_B = 0(\sigma^{-\frac{1}{4}}U_B)$ in both layers whereas u_F is $0(U_\infty)$ in the outer layer (as it must, in order to match the uniform stream at the outer edge) and $0(\sigma^{-\frac{1}{4}}U_\infty)$ in the inner layer.

Rotem and Claassen determined $\tilde{\Phi}_0$, $\tilde{\Theta}_0$ and $\tilde{\phi}_0$, whereas it is a simple matter to show that $\tilde{\phi}_1$ is governed by

$$\left.\begin{aligned} &\tilde{\phi}_1''' + \tfrac{3}{5}\tilde{\phi}_0\tilde{\phi}_1'' - \tfrac{1}{5}\tilde{\phi}_0'\tilde{\phi}_1' + \tfrac{2}{5}\tilde{\phi}_0''\tilde{\phi}_1 = 0, \\ &\tilde{\phi}_1'(\infty) = 1, \quad \tilde{\phi}_1(0) = 0 = \tilde{\phi}_1'(0), \end{aligned}\right\} \tag{29}$$

with $\tilde{\Phi}_1$ and $\tilde{\Theta}_1$ being determinable from:

$$\left.\begin{aligned} &\tilde{\Phi}_1''' = -\tfrac{1}{5}\int_\kappa^\infty \tilde{\Theta}_1 \, d\kappa - \tfrac{2}{5}\kappa\tilde{\Theta}_1, \\ &\tilde{\Theta}_1'' + \tfrac{3}{5}\tilde{\Phi}_0\tilde{\Theta}_1' + \tfrac{1}{5}\tilde{\Phi}_0'\tilde{\Theta}_1 + \tfrac{2}{5}\tilde{\Theta}_0'\tilde{\Phi}_1 = 0, \\ &\tilde{\Phi}_1(0) = 0 = \tilde{\Phi}_1'(0) = \Theta_1(0) = \Theta_1(\infty), \\ &\qquad\qquad \tilde{\Phi}_1''(0) = \phi_1''(0). \end{aligned}\right\} \tag{30}$$

It is noted that $\tilde{\phi}_1$ arises from the inhomogeneous matching condition in (29), representing the requirement that $u \sim U_\infty$ at the outer edge of boundary layer; in turn, $\tilde{\Phi}_1$ arises from the inhomogeneous matching condition in (30), indicating that the flow in the inner layer is dragged by the outer layer via viscous shear.

Previously-obtained numerical solutions (slightly corrected) by Rotem and Claassen show that

$$\left.\begin{aligned} &\tilde{\Phi}_0''(0) = 0{\cdot}97534, \quad \tilde{\Theta}_0'(0) = -0{\cdot}45619, \\ &\tilde{\Phi}_0(\kappa) \underset{\kappa\to\infty}{\sim} 1{\cdot}1488\kappa - 1{\cdot}0392, \\ &\tilde{\phi}_0(\infty) = 1{\cdot}5043, \end{aligned}\right\} \tag{31}$$

whereas numerical integration of (29) and (30) results in:

$$\left.\begin{aligned} &\tilde{\phi}_1(\omega) \underset{\omega\to\infty}{\sim} \omega - 2{\cdot}2807, \quad \tilde{\phi}_1''(0) = 0{\cdot}32672, \\ &\tilde{\Phi}_1''(0) = 0{\cdot}16484, \quad \tilde{\Theta}_1'(0) = -0{\cdot}042408. \end{aligned}\right\} \tag{32}$$

In summary, the above results for large σ indicate that, in the near region, u_B is $0(\varepsilon U_\infty/\sigma)$ in both layers whereas u_F is $0(U_\infty)$ in the outer layer but $0(U_\infty/\sigma^{\frac{1}{4}})$ in the inner, wherein $u_F \sim 0{\cdot}33206\, U_\infty \eta = 0{\cdot}33206\, U_\infty \xi/\sigma^{\frac{1}{4}}$. Therefore, the above perturbation expansion about the forced flow breaks down first in the inner layer, occurring in the region where $\varepsilon U_\infty/\sigma = 0(U_\infty/\sigma^{\frac{1}{4}})$, i.e. $x/\lambda = 0(\sigma^{\frac{1}{4}}/\gamma^2)$. Hence, as $\sigma \to \infty$, the near region (characterized by a forced-flow boundary-layer structure) corresponds to where

$$0(1) < \frac{x}{\lambda} < 0(\sigma^{\frac{1}{4}}/\gamma^2). \tag{33}$$

Clearly, in order that there be such a region, it is necessary that $\gamma < 0(\sigma^{\frac{1}{4}})$.

On the other hand, the far-region perturbation expansion about the natural-convection flow indicates that u_B is $0(U_B/\sigma^{\frac{1}{4}})$ in both layers of this region whereas u_F is $0(U_\infty)$ in the outer and $0(U_\infty/\sigma^{\frac{1}{4}})$ in the inner. Hence, in order that $u_F < 0(u_B)$ in both layers of the far-region boundary layer, it is necessary that $U_\infty < 0(U_B/\sigma^{\frac{1}{4}})$, i.e. $0(\sigma^3/\gamma^2) < x/\lambda$. Therefore, as $\sigma \to \infty$, the far region (characterized by a natural-convection boundary-layer structure) occurs where

$$0(\sigma^3/\gamma^2) < \frac{x}{\lambda}. \tag{34}$$

Of course, in order that the boundary-layer

approximation be valid, it is required also that $\delta_B \sigma^{\frac{1}{10}} < 0(x)$, i.e. $G > 0(\sigma^{\frac{1}{2}})$. But, in the region corresponding to (34), $G \equiv \gamma(x/\lambda)^3 > 0(\sigma^9/\gamma^5)$, which exceeds $0(\sigma^{\frac{1}{2}})$ provided $\gamma < 0(\sigma^{\frac{1}{2}})$, a constraint which is seen to be less restrictive than that required for the existence of the near region.

Hence, provided $\gamma < 0(\sigma^{\frac{1}{2}})$ as $\sigma \to \infty$, the flow in the near region defined by (33) is a forced-flow-dominated boundary layer and, in the far region defined by (34), the flow is a buoyancy-dominated boundary layer. Apparently, then, in the "intermediate region", where

$$0\left(\frac{\sigma^{\frac{1}{2}}}{\gamma^2}\right) \leqslant \frac{x}{\lambda} \leqslant 0\left(\frac{\sigma^3}{\gamma^2}\right), \tag{35}$$

neither the forced flow nor buoyancy dominates.

It can be shown, however, that throughout most of the intermediate region, namely,

$$0\left(\frac{\sigma^{\frac{1}{2}}}{\gamma^2}\right) < \frac{\alpha}{\lambda} < 0\left(\frac{\sigma^3}{\gamma^2}\right), \tag{36}$$

the outer layer is dominated by the forced flow (with a thickness of order $x/R^{\frac{1}{2}}$) whereas the inner layer is dominated by buoyancy (with a thickness of order $x/(\sigma G)^{\frac{1}{4}}$). In fact, appropriate perturbation expansions in the intermediate subregion defined by (36) are:

$$\left.\begin{aligned} \psi &\sim U_\infty \delta[\hat{\phi}_0(\eta) \\ &\quad + \hat{\varepsilon}\hat{\phi}_1(\eta) + \ldots], \\ T - T_\infty &\sim 0 \end{aligned}\right\} \begin{array}{l}\eta \text{ fixed} \\ \text{as } \sigma \to \infty\end{array} \tag{37}$$

$$\left.\begin{aligned} \psi &\sim U_B \delta_B \sigma^{-\frac{1}{2}}[\hat{\Phi}_0(\kappa) \\ &\quad + \varepsilon^*\hat{\Phi}_1(\kappa) + \ldots], \\ T - T_\infty &\sim \Delta T[\hat{\Theta}_0(\kappa) \\ &\quad + \varepsilon^*\hat{\Theta}_1(\kappa) + \ldots]. \end{aligned}\right\} \begin{array}{l}\kappa \text{ fixed} \\ \text{as } \sigma \to \infty\end{array} \tag{38}$$

The perturbation term in the outer layer, $\hat{\phi}_1$, is due to buoyancy and matches the leading-order term, $\hat{\Phi}_0$, of the inner whereas $\hat{\phi}_0$ is associated with the forced flow and matches $\hat{\Phi}_1$ of the inner. It is noted that $\hat{\varepsilon}$ increases with x, becoming 0(1) where $x/\lambda = 0(\sigma^3/\gamma^2)$, whereas ε^* decreases with x, being 0(1) where $x/\lambda = 0(\sigma^{\frac{1}{2}}/\gamma^2)$; therefore, the perturbation expansion in the outer layer, (37), breaks down at the end of the intermediate subregion, (36), whereas that in the inner, (38), does not become valid until the start of the subregion.

It may be verified that $\hat{\phi}_0(\eta)$ is merely the Blasius stream-function, $F_0(\eta)$, and that $\hat{\Phi}_0(\kappa)$ and $\hat{\Theta}_0(\kappa)$ are the same as $\tilde{\Phi}_0(\kappa)$ and $\tilde{\Theta}_0(\kappa)$, respectively, of the far region. On the other hand, the first-order perturbation terms are governed by:

$$\left.\begin{aligned} &\hat{\phi}_1''' + \tfrac{1}{2}\hat{\phi}_0\hat{\phi}_1'' - \tfrac{1}{5}\hat{\phi}_0'\hat{\phi}_1' + \tfrac{7}{10}\hat{\phi}_0''\hat{\phi}_1 = 0, \\ &\hat{\phi}_1'(\infty) = 0 = \hat{\phi}_1(0), \\ &\hat{\phi}_1'(0) = \hat{\Phi}_0'(\infty) = 1{\cdot}1488, \end{aligned}\right\} \tag{39}$$

$$\left.\begin{aligned} &\hat{\Phi}_1''' = -\tfrac{1}{10}\int_\kappa^\infty \hat{\Theta}_1 \, d\kappa - \tfrac{2}{5}\kappa\hat{\Theta}_1, \\ &\hat{\Theta}_1'' + \tfrac{3}{5}\hat{\Phi}_0\hat{\Theta}_1' + \tfrac{3}{10}\hat{\Phi}_0'\hat{\Theta}_1 \\ &\qquad = -\tfrac{3}{10}\hat{\Theta}_0'\hat{\Phi}_1, \\ &\hat{\Phi}_1'(0) = 0 = \hat{\Phi}_1(0) = \hat{\Theta}_1(\infty) = \Theta,(0) \\ &\hat{\Phi}_1''(\infty) = \hat{\phi}_0''(0) = 0{\cdot}33206. \end{aligned}\right\} \tag{40}$$

Numerical integration results in:

$$\hat{\phi}_1(\infty) = 3{\cdot}4595, \quad \hat{\Phi}_1''(0) = 0{\cdot}20114, \quad \hat{\Theta}_1'(0) = -0{\cdot}042476. \tag{41}$$

Based upon the results of this section, it follows that, in the limit $\gamma < 0(\sigma^{\frac{1}{2}})$ as $\sigma \to \infty$, the local Nusselt number is given by:

$$N \sim \begin{cases} R^{\frac{1}{2}}\sigma^{\frac{1}{4}}\left[0{\cdot}33872 + 0{\cdot}59649 \times \left(\dfrac{\gamma^2 R}{\sigma^{\frac{1}{2}}}\right)^{\frac{1}{4}} + \ldots\right], \\ \qquad 0(1) < \dfrac{x}{\lambda} < 0\left(\dfrac{\sigma^{\frac{1}{2}}}{\gamma^2}\right), \\ (G\sigma)^{\frac{1}{4}}\left[0{\cdot}45619 + 0{\cdot}042476 \times \left(\dfrac{\sigma^{\frac{1}{2}}}{\gamma^2 R}\right)^{\frac{1}{10}} + \ldots\right], \end{cases} \tag{42}$$

$$\left\{\begin{array}{l} 0\left(\dfrac{\sigma^{\frac{1}{4}}}{\gamma^2}\right) < \dfrac{x}{\lambda} < 0\left(\dfrac{\sigma^3}{\gamma^2}\right), \\ (G\sigma)^{\frac{1}{4}}\left[0{\cdot}45619 + 0{\cdot}042408 \times \left(\dfrac{\sigma^{\frac{1}{4}}}{\gamma^2 R}\right)^{\frac{1}{4}} + \ldots\right], \\ 0\left(\dfrac{\sigma^3}{\gamma^2}\right) < \dfrac{x}{\lambda}. \end{array}\right.$$

It is noted that, as far as the heat transfer is concerned, natural convection is dominant already in the intermediate subregion.

4. SMALL σ

As $\sigma \to 0$, the well-known limit of the forced-flow temperature is given by:

$$H_0(\eta;\sigma) \sim \begin{cases} (\pi)^{-\frac{1}{2}} \int_{\zeta}^{\infty} e^{-t^2/4}\, dt, \\ \qquad \zeta \text{ fixed as } \sigma \to 0, \\ 1 - \left(\dfrac{\sigma}{\pi}\right)^{\frac{1}{2}}\eta, \quad \eta \text{ fixed as } \sigma \to 0, \end{cases} \tag{43}$$

where $\zeta \equiv \sigma^{\frac{1}{4}}\eta$ and, it is noted, the thermal convection is negligible in the velocity boundary layer, $\eta = 0(1)$, but is the same order as the thermal diffusion in the outer layer, of order $\delta/\sigma^{\frac{1}{4}}$ in thickness, wherein the velocity is essentially that of the uniform stream.

In a straightforward manner, the buoyancy-induced stream-function in the outer layer is expressible as

$$F_1(\eta;\sigma) \sim \sigma^{-1} f_1(\zeta), \quad \zeta \text{ fixed as } \sigma \to 0 \tag{44}$$

where, denoting the outer temperature distribution in (43) as $h_0(\zeta)$,

$$\left.\begin{array}{l} \frac{1}{2}\zeta f_1'' - \frac{1}{2}f_1' = -\frac{1}{2}\int_{\zeta}^{\infty} h_0\, d\zeta - \frac{1}{2}\zeta h_0, \\ f_1'(\infty) = 0 = f_1(0). \end{array}\right\} \tag{45}$$

That is, viscous diffusion is negligible in the outer layer, the horizontal momentum balance being between the inertial effect and the buoyancy-induced pressure gradient. It is noted that u_B is now $0(\varepsilon U_\infty/\sigma^{\frac{1}{4}})$.

The solution to (45) is expressible in closed-form as

$$f_1(\zeta) = 1 - \operatorname{erfc}(\zeta/2) + (\pi)^{-\frac{1}{2}}\zeta\, e^{-\zeta^2/4} - \tfrac{1}{2}\zeta^2 \operatorname{erfc}(\zeta/2). \tag{46}$$

Hence, in particular, $f_1(\infty) = 1$ and $f_1'(0) = 2/\pi^{\frac{1}{2}}$, the latter indicating the necessity for a viscous inner layer in order to satisfy the non-slip condition at the surface.

An appropriate expansion for F_1 in the inner layer is

$$F_1(\eta;\sigma) \sim \sigma^{-\frac{1}{4}}\mathscr{F}_1(\eta), \quad \eta \text{ fixed as } \sigma \to 0, \tag{47}$$

where $\mathscr{F}_1$ is governed by:

$$\left.\begin{array}{l} \mathscr{F}_1''' + \frac{1}{2}F_0\mathscr{F}_1'' - \frac{1}{2}F_0'\mathscr{F}_1' + F_0''\mathscr{F}_1 \\ \qquad = -\frac{1}{2}\int_0^{\infty} h_0\, d\zeta, \\ \mathscr{F}_1(0) = 0 = \mathscr{F}_1'(0), \quad \mathscr{F}_1'(\infty) = f_1'(0). \end{array}\right\} \tag{48}$$

The right-hand side of (48), arising from the buoyancy effect in the outer layer, represents a favorable pressure gradient which is imposed upon the inner layer. Numerical integration results in:

$$\mathscr{F}_1''(0) = 1{\cdot}5285,$$

$$\mathscr{F}_1(\eta) \sim \frac{2}{\pi^{\frac{1}{2}}}\eta + 1{\cdot}4677 \quad \text{as } \eta \to \infty. \tag{49}$$

Concerning the temperature field, it follows that, in the outer layer,

$$H_1(\eta;\sigma) \sim \sigma^{-\frac{1}{4}}h_1(\zeta), \quad \zeta \text{ fixed as } \sigma \to 0, \tag{50}$$

where

$$\left.\begin{array}{l} h_1'' + \frac{1}{2}\zeta h_1' - \frac{1}{2}h_1 = -h_0' f_1, \\ h_1(\infty) = 0 = h_1(0). \end{array}\right\} \tag{51}$$

A closed-form solution is given by:

$$h_1(\zeta) = \left[\frac{1}{4\pi^{\frac{1}{2}}}\zeta^2 e^{-\zeta^2/4} - \frac{1}{2\pi^{\frac{1}{2}}} e^{-\zeta^2/4} - \tfrac{3}{4}\zeta\right] \times \operatorname{erfc}\left(\frac{\zeta}{2}\right) + \tfrac{1}{2}\zeta \operatorname{erfc}^2\left(\frac{\zeta}{2}\right) - \frac{1}{2\pi}\zeta e^{-\zeta^2/2} + \frac{1}{2\pi^{\frac{1}{2}}} e^{-\zeta^2/4}. \quad (52)$$

Hence, in particular, $h_1'(0) = -\frac{1}{4}$.

In the inner layer, an appropriate expansion is now

$$H_1(\eta;\sigma) \sim \mathscr{H}_1(\eta), \quad \eta \text{ fixed as } \sigma \to 0, \quad (53)$$

where

$$\mathscr{H}_1'''(\eta) = 0, \quad \mathscr{H}_1(0) = 0, \quad \mathscr{H}_1'(\infty) = h_1'(0), \quad (54)$$

i.e. the thermal convection is negligible. It follows that

$$\mathscr{H}_1(\eta) = -\tfrac{1}{4}\eta. \quad (55)$$

In the far region, as was shown by Rotem and Claassen [7], the natural-convection flow consists of an inviscid outer thermal boundary layer, corresponding to $\tilde{\eta} = 0(\sigma^{-\frac{1}{2}})$, and a viscous inner layer, corresponding to $\tilde{\eta} = 0(\sigma^{\frac{1}{10}})$, wherein thermal convection is negligible and the flow is driven by an imposed favorable pressure gradient arising from the buoyancy effect in the outer layer.

Appropriate asymptotic expansions for (6) are given in the outer layer by:

$$\psi \sim U_B\delta_B\sigma^{-\frac{1}{2}}[\tilde{f}_0(\tilde{\zeta}) + \sigma^{\frac{1}{2}}\tilde{\varepsilon}\tilde{f}_1(\tilde{\zeta}) + \ldots], \quad T - T_\infty \sim \Delta T[\tilde{h}_0(\tilde{\zeta}) + \sigma^{\frac{1}{2}}\tilde{\varepsilon}\tilde{h}_1(\tilde{\zeta}) + \ldots], \quad \tilde{\zeta} \text{ fixed as } \sigma \to 0 \quad (56)$$

and, in the inner layer, by:

$$\psi \sim U_B\delta_B\sigma^{-\frac{1}{10}}[\tilde{\mathscr{F}}_0(\tilde{\xi}) + \sigma^{\frac{1}{2}}\tilde{\varepsilon}\tilde{\mathscr{F}}_1(\tilde{\xi}) + \ldots], \quad T - T_\infty \sim \Delta T[\tilde{\mathscr{H}}_0(\tilde{\xi}) + \sigma^{\frac{1}{10}}\tilde{\varepsilon}\tilde{\mathscr{H}}_1(\tilde{\xi}) + \ldots], \quad \tilde{\xi} \text{ fixed as } \sigma \to 0 \quad (57)$$

Hence, in both layers, $u_B = 0(U_B/\sigma^{\frac{1}{2}})$ and $u_F = 0(U_\infty)$.

Rotem and Claassen determined $\tilde{f}_0$, $\tilde{h}_0$, $\tilde{\mathscr{F}}_0$ and $\tilde{\mathscr{H}}_0$ whereas, concerning the first-order perturbation terms, the governing equations in the outer layer are

$$\tfrac{3}{5}\tilde{f}_0\tilde{f}_1'' - \tfrac{1}{5}\tilde{f}_0'\tilde{f}_1' + \tfrac{2}{5}\tilde{f}_0''\tilde{f}_1 = -\tfrac{1}{5}\int_{\tilde{\zeta}}^{\infty}\tilde{h}_1\,d\tilde{\zeta} - \tfrac{2}{5}\tilde{\zeta}\tilde{h}_1,$$
$$\tilde{h}_1'' + \tfrac{3}{5}\tilde{f}_0\tilde{h}_1' + \tfrac{1}{5}\tilde{f}_0'\tilde{h}_1 + \tfrac{2}{5}\tilde{h}_0'\tilde{f}_1 = 0,$$
$$\tilde{f}_1(0) = 0 = \tilde{h}_1(0) = \tilde{h}_1(\infty), \quad \tilde{f}_1'(\infty) = 1, \quad (58)$$

and, in the inner layer,

$$\tilde{\mathscr{F}}_1''' + \tfrac{3}{5}\tilde{\mathscr{F}}_0\tilde{\mathscr{F}}_1'' - \tfrac{1}{5}\tilde{\mathscr{F}}_0'\tilde{\mathscr{F}}_1' + \tfrac{2}{5}\tilde{\mathscr{F}}_0''\tilde{\mathscr{F}}_1 = -\tfrac{1}{5}\int_0^{\infty}\tilde{h}_1\,d\tilde{\zeta},$$
$$\tilde{\mathscr{H}}_1''(\tilde{\xi}) = 0,$$
$$\tilde{\mathscr{F}}_1(0) = 0 = \tilde{\mathscr{F}}_1'(0) = \tilde{\mathscr{H}}_1(0),$$
$$\tilde{\mathscr{F}}_1'(\infty) = \tilde{f}_1'(0), \quad \tilde{\mathscr{H}}_1'(\infty) = \tilde{h}_1'(0). \quad (59)$$

Previously-obtained numerical solutions (slightly corrected) by Rotem and Claassen show that

$$\tilde{f}_0(\infty) = 1{\cdot}8009, \quad \tilde{f}_0'(0) = 1{\cdot}5774, \quad \tilde{h}_0'(0) = -0{\cdot}57574, \quad \tilde{\mathscr{F}}_0''(0) = 1{\cdot}2309,$$
$$\tilde{H}_0(\tilde{\eta};\sigma) \sim 1 - 0{\cdot}57574\sigma^{\frac{1}{2}}\tilde{\xi} \ (\tilde{\xi} \text{ fixed as } \sigma \to 0). \quad (60)$$

whereas numerical integration of (58) and (59) gives:

$$\tilde{f}_1(\tilde{\zeta}) \sim \tilde{\zeta} - 2{\cdot}657 \text{ as } \tilde{\zeta} \to \infty, \quad \tilde{f}_1'(0) = -0{\cdot}2045, \quad \tilde{h}_1'(0) = -0{\cdot}07692, \quad \tilde{\mathscr{F}}_1''(0) = -0{\cdot}1790, \quad \tilde{\mathscr{H}}_1(\tilde{\xi}) = -0{\cdot}07692\tilde{\xi}. \quad (61)$$

In summary, the above results for small σ show that, in both the inner and outer layers of the near region, u_B is $0(\varepsilon U_\infty/\sigma^{\frac{1}{2}})$ and u_F is $0(U_\infty)$. Therefore, the above perturbation expansion about the forced flow breaks down where $\varepsilon/\sigma^{\frac{1}{2}} = 0(1)$, i.e. $x/\lambda = 0(\sigma/\gamma^2)$. Also, in order that the boundary layer in the near region be

thin, it is necessary that $x/(\sigma R)^{\frac{1}{4}} < 0(x)$ i.e. $x/\lambda > 0(\sigma^{-1})$. Hence, as $\sigma \to 0$, the near region corresponds to where

$$0(1/\sigma) < \frac{x}{\lambda} < 0(\sigma/\gamma^2). \tag{62}$$

Clearly, in order that such a region occur, it is required that $\gamma < 0(\sigma)$.

On the other hand, the perturbation expansion about the natural-convection flow indicates that, in both layers of the far region, u_B is $0(U_B/\sigma^{\frac{1}{4}})$ and u_F is $0(U_\infty)$. Hence, in order that $u_F < 0(u_B)$, it is necessary that $U_\infty < 0(U_B/\sigma^{\frac{1}{4}})$, i.e. $0(\sigma/\gamma^2) < x/\lambda$. Also, in order that the boundary layer in this region be thin, it is required that $x/(G\sigma^2)^{\frac{1}{4}} < 0(x)$ or, equivalently, $x/\lambda > 0(\gamma^{-\frac{1}{2}}\sigma^{-\frac{1}{4}})$. It is seen that this latter constraint is less restrictive than the former since if $\gamma < 0(\sigma)$ then $0(\sigma/\gamma^2) > 0(\gamma^{-\frac{1}{2}}\sigma^{-\frac{1}{4}})$. Hence, in the limit $\gamma < 0(\sigma)$ as $\sigma \to 0$, the far region occurs where

$$0(\sigma/\gamma^2) < \frac{x}{\lambda}. \tag{63}$$

That is, provided $\gamma < 0(\sigma)$ as $\sigma \to 0$, the flow in the near region defined by (62) is a forced-flow-dominated boundary layer and, in the far region defined by (63), the flow is a buoyancy-dominated boundary layer. The intermediate region therefore corresponds to $x/\lambda = 0(\sigma/\gamma^2)$.

Based upon the results of this section, it follows that, in the limit $\gamma < 0(\sigma)$ as $\sigma \to 0$, the local Nusselt number is given by:

$$N \sim \begin{cases} (\sigma R)^{\frac{1}{4}}\left[\pi^{-\frac{1}{4}} + \frac{1}{4}\left(\frac{\gamma^2 R}{\sigma}\right)^{\frac{1}{4}} + \ldots\right], \\ 0\left(\frac{1}{\sigma}\right) < \frac{x}{\lambda} < 0\left(\frac{\sigma}{\gamma^2}\right), \\ (\sigma^2 G)^{\frac{1}{4}}\left[0{\cdot}57574 + 0{\cdot}07692 \times \left(\frac{\sigma}{\gamma^2 R}\right)^{\frac{1}{4}} + \ldots\right], \quad 0\left(\frac{\sigma}{\gamma^2}\right) < \frac{x}{\lambda}. \end{cases} \tag{64}$$

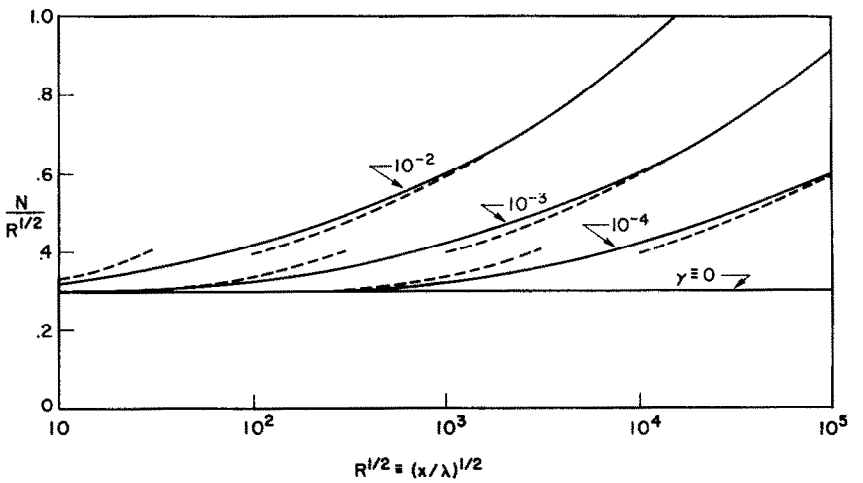

FIG. 2. Variation of $N/R^{\frac{1}{4}}$ vs. $R^{\frac{1}{4}}$ at $\sigma = 0{\cdot}72$ and various values of γ

5. DISCUSSION

As an application of the heat-transfer results presented in section 2, Fig. 2 shows the variation in the local Nusselt number along the plate for $\sigma = 0{\cdot}72$ and various values of γ; the dashed curves are based upon the first two terms of the near- and far-region results in (11), whereas the solid curves are based upon the dashed curve for $p(\chi)$ shown in Fig. 1. Figure 2 applies, e.g. to air at $\approx 20°C$, for which $\gamma \approx 0{\cdot}5\ \Delta T/U_\infty^3$ if ΔT is in °C and U_∞ in cm/s. Hence, if $\Delta T = 20°C$

and $U_\infty = 20$ cm/s then $\gamma \approx 10^{-3}$ and, based on Fig. 2, the buoyancy effect does not become significant until $R^{\frac{1}{2}} \approx 10^3$, a regime in which the assumption of laminar flow is somewhat untenable, turbulent transition occurring at $R \approx 10^6$ for the purely forced-flow situation. (The corresponding value for the mixed-convection problem is presumably smaller since the buoyancy gives rise to an inflection point in the velocity profile which, according to hydrodynamic stability theory, tends to lead to a less stable flow.) section 3, Fig. 3 shows the variation of the local Nusselt number along the plate for $\sigma = 10^3$ and various values of γ. The dashed curves are based upon the results obtained for the near region, intermediate subregion and far region (equation 42), the solid curve being drawn in via graphical interpolation. This figure is applicable, e.g. to light oil at $\approx 15°C$, for which $\gamma \approx 0{\cdot}5\ \Delta T/U_\infty^3$. Hence, if $\Delta T = 20°C$ and $U_\infty = 10$ cm/s then $\gamma \approx 10^{-2}$ and, based upon Fig. 3 (discounting the large viscosity variation

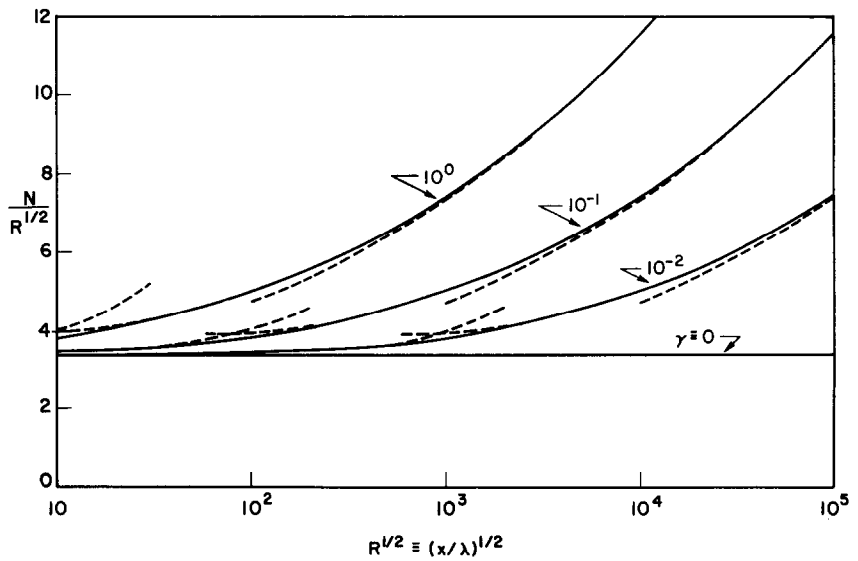

FIG. 3. Variation of $N/R^{\frac{1}{2}}$ vs. $R^{\frac{1}{2}}$ at $\sigma = 1000$ and various values of γ. Based on equation (42).

However, halving U_∞ to 10 cm/s results in $\gamma \approx 10^{-2}$ and, according to Fig. 2, the natural convection now becomes important where $R^{\frac{1}{2}} \approx 10^2$, i.e. during the early development of the laminar boundary layer. This clearly demonstrates that decreasing U_∞ while keeping all other quantities fixed causes the buoyancy-dominated region to move rapidly forward towards the leading edge, the value of R in the intermediate region being, in fact, proportional to U_∞^6.

Based upon the large-σ results obtained in which would attend such a ΔT), the buoyancy effect does not become important until $R^{\frac{1}{2}} \approx 10^4$, indicating that turbulent-transition of the forced-flow boundary layer would occur before the natural convection became significant. Comparison with the above results in air clearly indicates that, for given ΔT and U_∞, the effect of buoyancy is much larger in air than in light oil or, more generally, in gases than in large-σ liquids.

As an application of the small-σ results obtained in section 4, Fig. 4 shows the variation

in the local Nusselt number along the plate for $\sigma = 10^{-2}$ and various values of γ. The dashed curves are based upon the results obtained for the near and far regions (equation 64), the solid curves being drawn in via graphical interpolation. This figure is applicable, e.g. to liquid sodium at $\approx 100°C$, for which $\gamma \approx 0{\cdot}002\,\Delta T/U_\infty^3$. Hence, if $\Delta T = 20°C$ and $U_\infty = 10$ cm/s then $\gamma \approx 4 \times 10^{-5}$ and, based upon Fig. 4, the at a fixed R and G, the effect of buoyancy decreases monotonically as σ increases.

The latter property is a fundamental characteristic of mixed convection and is due to the fact that the temperature field contracts as σ increases (thereby reducing the region over which the buoyancy acts). This characteristic was noted by Sparrow and Minkowycz [4] in their numerical calculations for the near region and

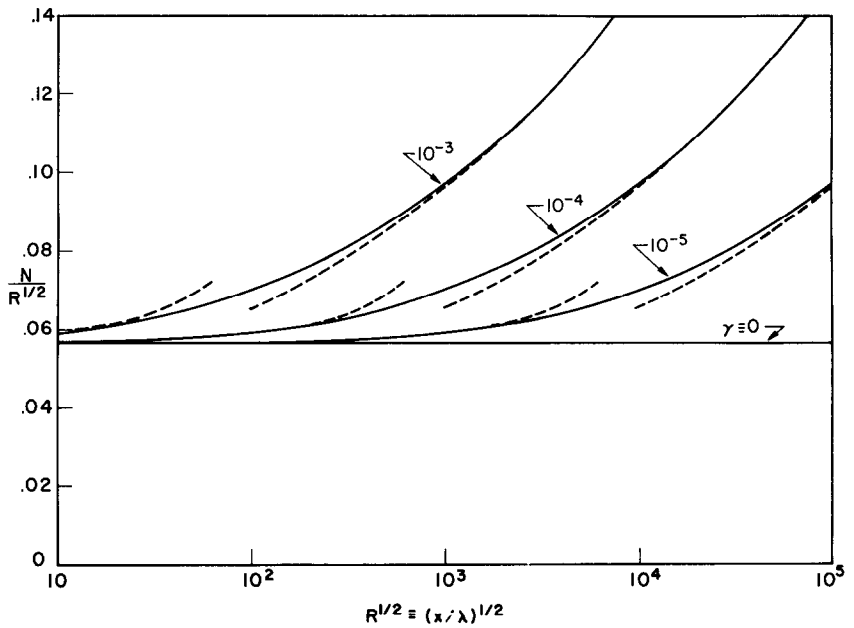

FIG. 4. Variation of $N/R^{\frac{1}{2}}$ vs. $R^{\frac{1}{2}}$ at $\sigma = 0{\cdot}01$ and various values of γ. Based on equation (64).

buoyancy effect does not become important until $R^{\frac{1}{2}} \approx 3000$, indicating that turbulent transition of the forced-flow boundary layer would occur before the natural convection became significant. Comparison with the above results in air indicates that, for given ΔT and U_∞, the effect of buoyancy is much larger in air than in liquid sodium or, more generally, in gases than in liquid metals. This result, which can be attributed to the relatively small kinematic viscosity and coefficient of thermal expansion of liquid metals, is somewhat unexpected since, can be seen most readily from the present analysis by noting that the buoyancy-induced velocity in the near region is of order $\varepsilon U_\infty \sigma^{-1}$ as $\sigma \to \infty$ but of order $\varepsilon U_\infty \sigma^{-\frac{1}{2}}$ as $\sigma \to 0$. Alternatively, this σ-dependence is shown in Fig. 5 in terms of the heat-transfer results obtained in sections 2–4. The "forced-convection regime" ("natural-convection regime") is that in which the local heat transfer due to the forced flow (buoyancy) is at least ten times as large as that due to the buoyancy (forced flow). Concerning the upper bound of the forced-convec-

tion regime, it is seen that the results of Sparrow and Minkowycz merge well with the large- and small-σ results of the present paper. The lower bound of the natural-convection regime has been sketched in on the basis of the large- and small-σ asymptotes of sections 3 and 4, together with the particular result at $\sigma = 0{\cdot}72$ obtained in section 2.

In applying Fig. 5 to particular instances, it is cautioned that the indicated constraint on γ be checked in order to assure that a forced-flow-dominated boundary-layer region is indeed present. Specifically, since δ_{th} characterizes the thickness of the boundary layer when $\sigma \leqslant 0(1)$, until $R^{\frac{1}{2}} \gtrsim 177$; therefore, since $\gamma R^{\frac{1}{2}} \approx 0{\cdot}017$ at $\sigma = 0{\cdot}01$ on the lower curve of Fig. 5, it follows that it is necessary that $\gamma \lesssim 0{\cdot}017/177 \approx 10^{-4}$ in order that there exist a forced-flow-dominated boundary-layer region when $\sigma = 0{\cdot}01$. (This indicates that the lower asymptotic behavior of the $\gamma = 10^{-3}$ curve in Fig. 4 is questionable.) Similarly, at $\sigma = 0{\cdot}72$ it is necessary that $\gamma \lesssim 0{\cdot}002$. For large σ, since the thickness of the boundary layer is not characterized by δ_{th} but rather by the displacement thickness, δ^*, it is required that $\delta^*/x \lesssim 0{\cdot}1$, say. Application of this to the forced-flow boundary layer ($\delta^* \approx 1{\cdot}72\ x/R^{\frac{1}{2}}$) indicates that, as $\sigma \to \infty$, the

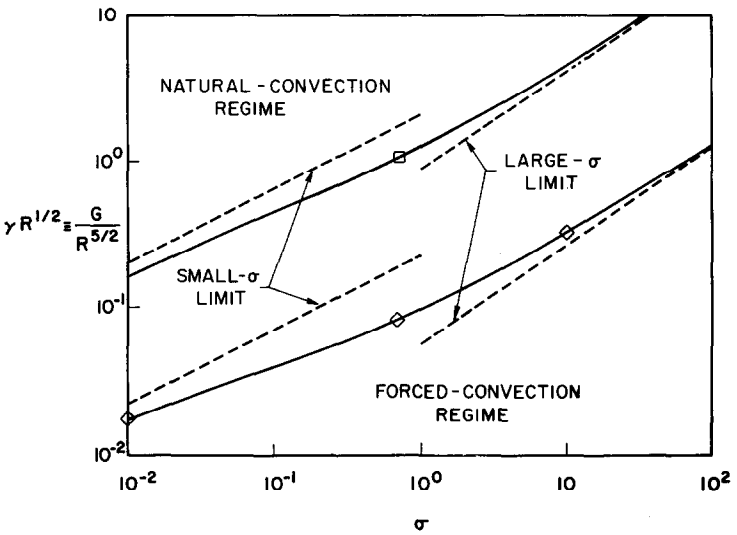

FIG. 5. The forced-convection and natural-convection heat-transfer regimes in terms of $\gamma R^{\frac{1}{2}}$ and σ. Numerical solutions: "◇", Sparrow and Minkowycz [4]; "□", section 2; large-σ limit, section 3; small-σ limit, section 4.

for this case a simple requirement for the existence of a boundary layer is that $\delta_{th}/x \lesssim 0{\cdot}1$, say. Applying this to be forced-flow boundary layer gives $R^{\frac{1}{2}} \gtrsim 17{\cdot}70\ \sigma^{-\frac{1}{2}}$ as $\sigma \to 0$ and $R^{\frac{1}{2}} \gtrsim 33{\cdot}8$ when $\sigma = 0{\cdot}72$. Hence, e.g. if $\sigma = 0{\cdot}01$ then a forced-flow boundary layer does not develop two-layer structure does not develop until $R^{\frac{1}{2}} \gtrsim 17{\cdot}2$. Hence, noting that $\gamma R^{\frac{1}{2}} \approx 1{\cdot}3$ at $\sigma = 10^2$ on the lower curve in Fig. 5, it follows that it is necessary that $\gamma \lesssim 1{\cdot}3/17{\cdot}2 \approx 0{\cdot}1$ in order that there exist a forced-flow-dominated boundary-layer region when $\sigma = 100$.

REFERENCES

1. A. A. SZEWCZYK, Combined forced and free convection laminar flow, *J. Heat Transfer* **86**, 501–507 (1964).
2. J. H. MERKIN, The effect of buoyancy forces on the boundary-layer flow over a semi-infinite vertical flat plate in a uniform free stream, *J. Fluid Mech.* **35**, 439–450 (1969).
3. Y. MORI, Buoyancy effects in forced laminar convection flow over a horizontal flat plate, *J. Heat Transfer* **83**, 479–482 (1961).
4. E. M. SPARROW and W. J. MINKOWYCZ, Buoyancy effects on horizontal boundary-layer flow and heat transfer, *Int. J. Heat Mass Transfer* **5**, 505–511 (1962).
5. K. STEWARTSON, On the free convection from a horizontal plate, *Z.A.M.P.* **9**, 276–282 (1958).
6. W. N. GILL, D. W. ZEH and E. DEL-CASAL, Free convection on a horizontal plate, *Z.A.M.P.* **16**, 539–541 (1965).
7. Z. ROTEM and L. CLAASSEN, Natural convection above unconfined horizontal surfaces, *J. Fluid Mech.* **39**, 173–192 (1969).
8. K. STEWARTSON, On asymptotic expansions in the theory of boundary layers, *J. Math. Phys.* **36**, 173–191 (1957).
9. I. IMAI, Second approximation to the laminar boundary-layer flow over a flat plate, *J. Aero. Sci.* **24**, 155–156 (1957).

CONVECTION MIXTE AU DESSUS D'UNE SURFACE CHAUFFEE HORIZONTALE

Résumé—Des effets d'Archimède sont déterminés analytiquement pour la région de la couche limite laminaire au-dessus d'une surface horizontale semi-infinie chauffée isothermiquement et placée dans un écoulement uniforme horizontal. On a déterminé les conditions de l'écoulement pour lesquelles la couche limite consiste en une région proche dominée par l'écoulement forcé et une région éloignée dominée par l'effet d'Archimède, séparées par une région intermédiaire où les convections forcée et naturelle sont d'importance comparable. On a obtenu les développements de la perturbation pour les régions proche et éloignée ainsi que des résultats, pour la région intermédiaire, obtenus par interpolation graphique.

Bien que l'on sache que pour des nombres fixés de Reynolds et de Grashof, l'effet d'Archimède décroît de façon monotone quand le nombre de Prandtl augmente, on a trouvé dans le présent problème que pour U_∞ et ΔT fixés, l'effet de convection naturelle est plus important dans les gaz que dans les huiles à grand σ ainsi que dans les métaux liquides à petit σ; ceci est dû à la viscosité cinématique relativement petite et au coefficient de dilatation thermique des métaux liquides. En tout cas, si $\Delta T \leqslant 20°C$, U_∞ doit alors être tout à fait petit ($\leqslant 20$ cm/s) si les effets d'Archimède doivent devenir significatifs avant que ne se produise la transition turbulente.

La présentation des résultats théoriques, $G/R^{5/2}$ en fonction de σ, conduit à une démarcation claire entre les régimes de transfert thermique par convection forcée, par convection mixte et par convection naturelle.

MISCHKONVEKTION ÜBER EINER BEHEIZTEN HORIZONTALEN OBERFLÄCHE

Zusammenfassung—Auftriebseffekte wurden analytisch bestimmt für den laminaren Grenzschichtbereich über einer isotherm beheizten halbunendlichen horizontalen Oberfläche, die in einer horizontalen gleichmässigen Strömung liegt.

Die Strömungsbedingungen wurden bestimmt, für welche die Grenzschicht in einen wandnahen erzwungenen Konvektionsbereich und einen entfernteren freien Konvektionsbereich eingeteilt werden kann; dazwischen liegt ein Gebiet, in dem erzwungene und natürliche Konvektion von vergleichbarer Größe sind. Störungsexpansionen erhält man für die nahen und fernen Gebiete mit den Ergebnissen für das dazwischenliegende Gebiet durch graphische Interpolation. Obwohl bekannt ist, dass bei festen *Re*- und *Gr*-Zahlen der Auftriebseffekt in gleichem Masse abnimmt wie die Prandtl-Zahl ansteigt, wurde für das vorliegende Problem gefunden, dass für feste U_∞ und ΔT der Einfluss der natürlichen Konvektion in Gasen nicht nur bedeutender als in Ölen mit großem *Pr* ist, sondern auch in Flüssigkeiten mit kleinem *Pr*. Das ist zurückzuführen auf die relativ kleine kinematische Zähigkeit und die thermischen Ausdehnungskoeffizienten flüssiger Metalle. Für $\Delta T \lesssim 20°C$ muß U_∞ klein sein ($\lesssim 20$ cm/s), wenn Auftriebeseffekte bedeutend werden sollen, ehe turbulenter Überschlag auftritt. Die Darstellung der theoretischen Ergebnisse in Gliedern von $G/R^{5/2}$ gegen *Pr* führt zu einer klaren Abgrenzung zwischen erzwungener, gemischter und natürlicher Konvektion.

СМЕШАННАЯ КОНВЕКЦИЯ НАД НАГРЕТОЙ ГОРИЗОНТАЛЬНОЙ ПОВЕРХНОСТЬЮ

Аннотация—Аналитически рассчитывалась сила плавучести в области ламинарного пограничного слоя над изотермически нагретой полуограниченной горизонтальной поверхностью в горизонтальном однородном потоке. Определялись условия, при которых пограничный слой состоит из ближнего участка с преобладающим вынужденным потоком и дальнего с доминирующей силой плавучести, между которыми находится промежуточная зона, где вынужденная и естественная конвекция сравнимы. По теории возмущений получены разложения для ближнего и дальнего участков, причем результаты для промежуточной зоны получены путем графической интерполяции.

Хотя хорошо известно, что при фиксированных значениях чисел Рейнольдса и Грасгофа эффект плавучести монотонно уменьшается с увеличением числа Прандтля, что для данной задачи, то есть для фиксированных значений U_∞ и ΔT, влияние естественной конвекции более значительно в газах не только по сравнению с маслами при больших значениях σ, но также и с жидкостями при малых значениях σ. Это объясняется сравнительно небольшими кинематической вязкостью и коэффициентом теплового расширения жидких металлов. В любом случае, если $\Delta T \lesssim 20^\circ$C, величина U_∞ должна оыть совсем небольшой, чтобы силы плавучести стали значительными до наступления турбулизации потока.

Теоретические результаты, представленные в виде зависимости $G/R^{5/2}$ от σ, ведут к чёткому разграничению режимов теплообмена с вынужденной, смешанной и естественной конвекцией.